

Performance Analysis of a Reuse Partitioning Technique for OFDM Based Evolved UTRA

Gábor Fodor, Ericsson Research

Abstract—The current 3GPP working assumption on the Evolved Universal Terrestrial Radio Access (E-UTRA) physical layer is that it will be based on single carrier frequency division multiple access (SC-FDMA) for the uplink and orthogonal frequency division multiple access (OFDMA) for the downlink. According to the concept specification, inter-cell interference mitigation techniques applicable to SC-FDMA and OFDMA systems are expected to be the key radio resource management techniques for E-UTRA. In this paper we propose and analyze a simple reuse partitioning technique (assuming coordinated sub-carrier allocation in the cells) that is able to minimize inter-cell interference. We propose a model that is able to take into account that sessions dynamically enter and leave the system. Rigid sessions require a class-specific fixed number of sub-carriers, while elastic sessions can enter the system if a minimum number of sub-carriers is allocated to them. In this rather general setting we analyze the system performance in terms of the expected number of sub-carrier collisions, the session blocking probabilities and the signal-to-noise-and-interference ratio performance. We present numerical results on the various trade-offs between these measures that provide insight into the behavior of OFDM based cellular systems and help dimension the parameters of a reuse partitioned system.

I. INTRODUCTION

On-going work within the 3rd Generation Partnership Project (3GPP) has recently proposed the use of single carrier frequency division and orthogonal frequency division as the means for multiple access in evolved Universal Terrestrial Radio Access (E-UTRA) systems [1]. An important characteristic of both types of multiple access techniques is that they are able to provide orthogonality and thereby nearly eliminate intra-cell interference within a single cell. However, sub-carriers (sometimes referred to as channels) in neighbor cells can cause significant interference to one another unless sophisticated inter-cell interference mitigation techniques are applied. Therefore, the 3GPP is currently studying inter-cell interference mitigation techniques including interference coordination/avoidance, interference randomization and interference cancellation (see Section 7.1.2.6 and Section 9.1.2.7 of [1] for details). A promising candidate that has been used in various other wireless technologies is *reuse partitioning* (see for instance [8] and the references therein) that provides a tool to control the reuse factor in different parts of a cell. (See also Figure 1 and Figure 2.)

One of the key drivers for the evolution of UTRA is the desire to support high bit-rate data services, including so called *rigid* or peak allocated and *elastic* ones whose bit-rate can be dynamically adjusted during their residency time in the system [2]. The integration of these types of services in a code division multiple access environment has been in the

focus of the seminal paper by Altman [5] (see also [6] and [7]) that proposes a Shannon-like capacity measure to characterize the capacity of such systems. A key result of that paper has been that the Erlang capacity of CDMA cellular systems increases if elastic sessions tolerate a higher *slowdown* of their bit-rates. This result is non-trivial, because although slowing down the session bit-rates to an accepted minimum value obviously increases the number of accommodated sessions, but it also increases the holding time of the sessions. When elastic sessions in OFDMA systems are present, we expect that the system capacity depends not only on the interference mitigation techniques, but also on the Altman-like trade-off between the allocated bit-rates and the session holding times. Therefore, there is a strong desire both from a system design and from a theoretical point of view to understand the behavior of the system when applying different radio resource management techniques in the presence of elastic traffic. Specifically, there is an interest in analyzing the impact of various interference mitigation techniques applicable in OFDMA on the system capacity when some portion of the carried traffic is elastic. To our best knowledge, this issue has not yet been analyzed in the literature.

Therefore, the purpose of the current paper is to develop a model and methodology to analyze the performance of OFDMA based cellular systems under various interference mitigation techniques that are realistic from a system design perspective (see for instance [3] for a discussion on the control plane aspects). Typically, such interference management techniques co-exist with other radio resource management (RRM) techniques, such as admission control and rate allocation; therefore our purpose is to understand the impact of these techniques when they are applied together.

The paper is structured as follows. The next Section presents our basic model for an E-UTRA system, where we assume that there is a single dominant interfering cell to the cell under study. Next, in Section III we analyze two interference mitigation techniques and compare their performance in terms of their associated sub-carrier (channel) collision probabilities. Subsequently, we consider the situation in which sessions dynamically arrive and leave the system when assuming rigid and elastic traffic types. This section highlights the trade-off between blocking probabilities and the mean number of sub-carrier collisions. Section IV provides a method to analytically calculate the probability that the signal-to-noise-and-interference ratio (SINR) exceeds a predefined threshold; this type of analysis may provide input to link level models and help evaluate the symbol loss probabilities. The numerical

results of this section provide insight into the trade-off between the session-wise blocking probabilities and the SINR values under different interference mitigation techniques. Finally, based on the numerical results, in Section V we discuss the pros and cons of interference mitigation techniques for E-UTRA.

II. REUSE PARTITIONING WITH COORDINATED SUB-CARRIER ALLOCATION

A. Basic Considerations

The basic concept of reuse partitioning along with the model parameters are presented in Figure 1 and Figure 2. In a Reuse-1 system, the entire frequency band is reused in every cell of the coverage area. In contrast, in a Reuse- n system the available frequency resources are divided between a group of n cells, such that frequency domain collisions within the group (i.e. neighbor cells using sub-carriers of exactly the same frequency at the same time) are avoided. This can be achieved in an arrangement, in which some sub-carriers in each cell are barred (taken out of use) so that in each cell there is a subset of the available sub-carriers that are not used by neighbor cells. In the two-cell system of Figure 1 and 2, R_0 and R_1 out of the available CH sub-carriers (channels) are barred in Cell-0 and Cell-1 respectively. Under the *reuse partitioning* allocation policy, the coverage area of a single cell is divided into several regions, each region having its own reuse factor. Reuse partitioning (see Figure 2) obviously increases the resource utilization within each cell (as compared to the non-partitioned reuse system), since now mobile stations in the interior area may make use of the entire frequency band. It follows that the three key parameters of a partitioned system are (1) the location of the border line between the interior and exterior areas, (2) the number of restricted sub-carriers that can only be used by mobile stations in the interior area and (3) the applied sub-carrier power levels by interior and exterior mobile stations. The first two aspects are studied in this and the next Section, while the third aspect is the topic of Section IV.

B. Mean Number of Collisions under Coordinated Sub-carrier Allocation with/without Reuse Partitioning

Basically, there are two approaches as to *how* the sub-carriers out of the available ones are selected when a session requires a certain number of sub-carriers. The simplest is way is to pick sub-carriers out of the ones that are available randomly such that any available sub-carrier has the same probability to get allocated to an arriving session. *Random allocation* of sub-carriers is attractive, because it does not require any coordination between cells, but it may cause collisions even when there are free sub-carriers. In contrast, a low complexity coordination can avoid collisions as long as there are non-colliding sub-carrier pairs in the two cells. We refer to this method as *coordinated* sub-carrier allocation. In this paper we focus on coordinated allocation and refer to [4] for an analysis of the random allocation technique.

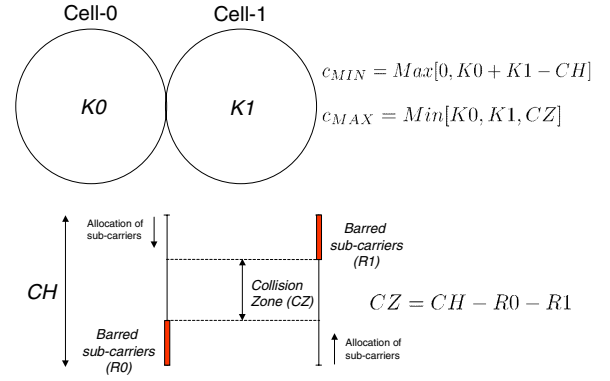


Fig. 1. A two-cell OFDMA system with CH number of sub-carriers in each cell with *coordinated* sub-carrier allocation without reuse partitioning. In each cell, a certain number of sub-carriers (R_0 and R_1 respectively) may be taken out of use so that sub-carrier collisions are only possible in the *collision zone* (CZ). The number of non-used sub-carriers present a trade-off between the collision probability and the resource utilization in the cells.

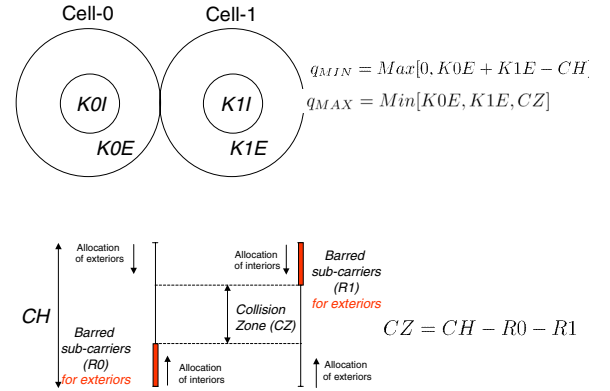


Fig. 2. A two-cell OFDMA system with CH number of sub-carriers in each cell with *coordinated* sub-carrier allocation with reuse partitioning. In this scheme, the system distinguishes between the *interior* and *exterior* parts of the cells. Only the collisions between exterior sub-carriers are considered as ones that cause inter-cell interference to one another. Therefore, all sub-carriers can be allocated to sessions of user equipments that are located in the interior of the cells.

For the case with coordinated allocation without reuse partitioning, the following lemma establishes the mean number of collisions when the number of allocated sub-carriers is K_0 and K_1 in the two cells.

Lemma 1: The mean number of collisions (γ_1) is given by:

$$E[\gamma_1|K_0, K_1] = \sum_{c=c_{MIN}}^{c_{MAX}} \frac{c \cdot N1(c)}{TOT1}, \quad TOT1 = 1, \quad \text{and}$$

$$N1(c) = \begin{cases} 1 & \text{if } c = c_0 \\ 0 & \text{otherwise.} \end{cases} \quad (1)$$

where

$$c_0 = \text{Min}[\text{Max}[0, (K_0 + K_1 - CH)], K_0, K_1, CZ].$$

Proof: Because of the coordinated (deterministic) allocation procedure, collisions will only occur when the number of allocated sub-carriers in the two cells ($K_0 + K_1$) exceeds the number of available ones (CH). On the other hand, the

number of collisions is obviously limited by the collision zone. $N1(c)$ gives the number of possible allocations such that the number of collisions is c . $TOT1$ gives the number of possible allocations and $N1(c)/TOT1$ is the probability that in the coordinated sub-carrier allocation case the number of collisions is c . ■

For the reuse partitioning case we can calculate the mean number of collisions in a similar way. In this case, one is interested in the number of "real" collisions, that is collisions between mobile stations in the exterior area of the cell (implicitly assuming that collisions caused by interior mobile stations do not cause noticeable impact on the SINR performance; this issue is examined in Section IV).

Lemma 2: Using similar notations as in Lemma 1, the mean number of "real" collisions" (γ_2) is given by:

$$E[\gamma_2|K0E, K0I, K1E, K1I] = \sum_{q=q_{MIN}}^{q_{MAX}} \frac{q \cdot N2(q)}{TOT2},$$

$$TOT2 = 1,$$

$$N2(q) = \begin{cases} 1 & \text{if } q = q_0 \\ 0 & \text{otherwise.} \end{cases} \quad (2)$$

where $q_0 =$

$$\text{Min} \left[\text{Max}[0, (K0E + K1E - CH)], K0E, K1E, CZ \right].$$

Proof: A similar reasoning as in the previous case applies, but now we have to take into account that collisions occur only between external sub-carriers. (That is sub-carriers allocated to mobile stations in the exterior area of the cells.) ■

C. A Numerical Example

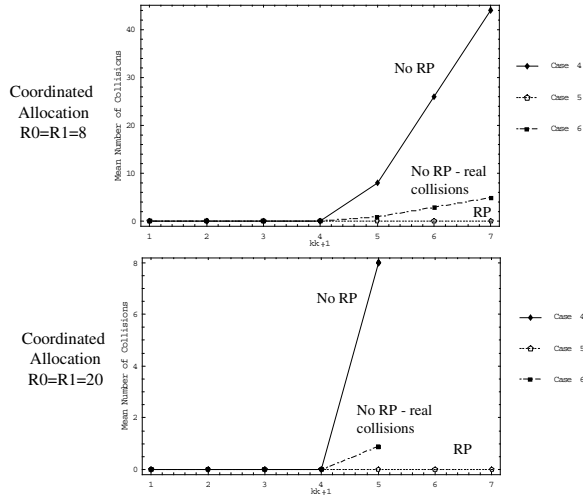


Fig. 3. Mean number of sub-carrier collisions as the function of the coordinated allocated sub-carriers. Increasing the $R0$ and $R1$ helps reduce the collisions, but when kk reaches 5 ($K0 = K0E + K0I = K1 = K1E + K1I = kk * 9 = 45$), in the $R0 = R1 = 20$ case the non-partitioned system ("No RP") cannot accommodate the required amount sub-carriers, since $CH - R0 = CH - R1 = 44 < 45$. When reuse partitioning is applied, the number of accommodated sub-carriers increases.

For illustration purposes, consider a simple case with $CH = 64$ with coordinated (Figure 3) sub-carrier allocation. In each

cell, $R = R0 = R1$ sub-carriers are restricted to be allocated for interior sessions ($R = 8$ and $R = 20$), therefore without reuse partitioning (Case 1) only 56 or 44 channels may be used in each cell. With reuse partitioning (Case 2), all channels can be used, but the restricted ones only by mobile stations located in the interior part of the cell. We use "Case 3" to refer to the arrangement and allocation method of Case 1, but now only taking into account the collisions that would be classified as collisions between two external mobiles if we distinguished between exterior and interior areas; that is Case 3 counts the "real" collisions in the non-partitioned case.

With coordinated allocation but without reuse partitioning, the system does not distinguish between interior and exterior sessions; the available sub-carriers are allocated one after the other starting from the "top" in Cell-0 and from the "bottom" in Cell-1. When there are $K > R$ allocated sub-carriers, $K - R$ of these will be in the collision zone (Figure 3, Case 1 curve). But the "real" collisions are only those that happen between exterior sessions, whose number will depend on how many out of the exterior ones will collide in the collision zone ("Case 1 real collisions"). Under reuse partitioning, when the allocation procedure distinguishes between mobile stations in the interior and exterior areas of the cells, it is possible to allocate the sub-carriers such that none of the exterior sub-carriers collide ("Case 2"). "Case 3" refers to the arrangement and allocation method of Case 1, but now only taking into account the collisions that would be classified as collisions between two external mobiles if we distinguished between exterior and interior areas; that is Case 3 counts the "real" collisions in the non-partitioned case. It is important to note that the coordination between cells can be achieved by a predefined cell-specific scheme that specifies a certain order in which the sub-carriers are taken into use. In practice, such an ordering scheme could be quasi-static in order to avoid excessive run-time signaling.

III. MODELING DYNAMIC SESSION ARRIVALS AND ADMISSION CONTROL

The lemmas in the preceding Section provide insight into how the collision probabilities depend on the allocation strategies given that the number of allocated sub-carriers is known in each cell. In real systems, the number of allocated sub-carriers depends on the number of in-progress sessions and on the number of sub-carriers that are allocated to each session. Obviously, the number of on-going sessions depends on the arrival and departure process and also on the admission control strategy, while the number of allocated sub-carriers to each session depends on the assigned instantaneous rate allocations. In order to proceed, we will make some assumptions that restrict our focus on a practically relevant case rather than modeling the admission control and rate assignment algorithms in their generality. We believe that these assumptions can be modified to other practically relevant cases as well. First, we assume that sessions arrive according to Poisson processes with a class specific arrival intensity λ_i . We will also assume that the session holding times are exponentially

distributed random variables with mean value $1/\mu_i$ if the session is served at its required peak rate.

When sessions arrive and leave dynamically, let the quadruple $(U_1, U_2, U_3, U_4) \equiv (U_{0,r}, U_{0,e}, U_{1,r}, U_{1,e})$ be the *state* of the system, where the elements of the quadruple denote the number of real time (Class-1 and Class-3) and elastic (Class-2 and Class-4) sessions in Cell-0 and Cell-1 respectively.¹ The number of sub-carriers that need to be allocated to Class-1 and Class-3 (peak allocated or "rigid") sessions is denoted by $l_1 = l_3 \equiv l_r$. If, at the time of arrival of a rigid session, this amount of sub-carriers cannot be allocated, the session is rejected (blocked) and leaves the system. In contrast, elastic sessions from Class-2 and Class-4 tolerate a certain *slowdown* of their bit-rates ([5]) which corresponds to the situation in which the number of sub-carriers allocated is reduced from $l_2^{MAX} = l_4^{MAX} \equiv l_e^{MAX}$ to $l_2^{MIN} = l_4^{MIN} \equiv l_e^{MIN}$. In other words, l_e^{MAX} and l_e^{MIN} correspond to the required number of sub-carriers when sending with the peak and the minimum (in 3GPP parlance: guaranteed) bit-rates respectively. The $\hat{a}_2 = \hat{a}_4 = l_e^{MAX}/l_e^{MIN}$ value represents the maximum slowdown factor of the elastic sessions.

We now need to determine the feasible states of the system and to establish the number of allocated sub-carriers to rigid and elastic sessions in each state. We also need to know the slowdown factors for elastic sessions in each system state, since these determine the holding time of elastic sessions and thereby have an impact on the steady state distribution of the system.

A. Performance Measures of Interest

In this dynamic case, the primary performance measures of interest are the class-wise blocking probabilities and the expected number of collisions. In addition, since slowing down the bit-rates implies an increased holding time (a decreased class-wise throughput), the mean holding time and the throughput are also of interest. Finally, since the operator revenue is directly related to the average number of sessions in the system, we are also interested in that measure.

B. Determining the State Space of the System

In the following we will make the assumptions that all rigid (peak allocated) sessions are born in the interior area, while all elastic sessions arrive in the exterior area. This assumption basically says that interior sessions are peak allocated, while exterior sessions tolerate a certain slowdown of their peak bit-rates. The rationale behind this assumption is that mobile stations close to their own (serving) base stations cause less interference to surrounding cells than mobile stations closer to the cell edge. Actually, this assumption could be easily relaxed such that both interior and exterior sessions can be rigid and elastic ones at the expense of increasing the state variables to eight (from the currently used quadruple).

¹Although the system supports two service classes (one peak allocated and one elastic class), we talk about *four* classes in order to distinguish between Cell-0 and Cell-1 classes.

For ease of notation and to be able to handle Case 1 and Case 2 uniformly, we introduce the terms $R0I$ and $R1I$ that give the number of sub-carriers that cannot be allocated to mobile stations that are in the interior area. Obviously, $R0I = R0$ and $R1I = R1$ in Case 1 (when there is no reuse partitioning, the $R0$ and $R1$ restrictions apply to both the interior and the exterior sessions), while $R0I = R1I = 0$ in Case 2 (reuse partitioning).

We first define the set of feasible states (or state space) of this system. The state space consists of the quadruples for which there exists a rate allocation such that the class-wise minimum bit-rate requirements can be satisfied with the available system resources:

$$\mathcal{S} = \left(\underline{U} : \exists l_2, l_4 : l_e^{MIN} \leq l_2, l_4 \leq l_e^{MAX}; \right. \\ \left. \sum_{k=1}^2 U_k \cdot l_k \leq CH - (R0 - R0I); \right. \\ \left. \sum_{k=3}^4 U_k \cdot l_k \leq CH - (R1 - R1I) \right).$$

Then, the maximum number of rigid (all interior) sessions is $U_{i,r}^{MAX} = \lfloor \frac{CH - RiI}{l_r} \rfloor$; $i = 0, 1$. The maximum number of real time sessions in the restricted zone (that is the sessions that can make use of the $R0$ and $R1$ sub-carriers) is $U_{0,r}^{R0I} = \frac{R0 - R0I}{l_r}$ and $U_{1,r}^{R1I} = \frac{R1 - R1I}{l_r}$. We will assume that $U_{0,r}^{R0I}$ and $U_{1,r}^{R1I}$ are integer numbers; we believe that this assumption is not restrictive, because (at least in this two-class case) knowing l_r it is possible to choose $R0$ and $R1$ such that this assumption holds.

Next, we make use of the characteristics of the sub-carrier allocation in Case 4 and Case 5: the allocation is such that the real time sessions are allocated sub-carriers from among the $R0$ and $R1$ restricted ones as long as there is any such still available. Under this assumption, the maximum number of elastic sessions ($U_{i,e}^{MAX}$) satisfies:

$$U_{i,e}^{MAX} \cdot l_e^{MIN} + (U_{i,r} - U_{i,r}^{RiI}) \cdot l_r \leq CH - Ri; \\ U_{i,r} = 0 \dots U_{i,r}^{MAX}; \quad i = 0, 1. \quad (3)$$

Since $U_{i,r}^{MAX}$ is known, equation (3) helps determine the feasible state space, since for each $U_{i,r}$, the value of $U_{i,e}^{MAX}$ can now be determined:

$$U_{i,e}^{MAX} = \left\lfloor \frac{CH - Ri - (U_{i,r} - U_{i,r}^{RiI}) \cdot l_r}{l_e^{min}} \right\rfloor; \\ U_{i,r} = 0 \dots U_{i,r}^{MAX}. \quad (4)$$

Equation (4) determines the set of quadruples (the *feasible* states) that constitute the \mathcal{S} state space of the system. We now need to calculate the maximum number of elastic sessions such that each elastic session receives the maximum number of sub-carriers (i.e. no slowdown $U_{i,e}^{small}$). This is straightforward, since:

$$U_{i,e}^{small} \cdot l_e^{MAX} + (U_{i,r} - U_{i,r}^{RiI}) \cdot l_r < CH - RiI;$$

$$U_{i,e}^{small} = \left\lfloor \frac{(CH - RiI) - (U_{i,r} - U_{i,r}^{RiI})}{l_e^{MAX}} \right\rfloor.$$

If there are more than $U_{i,e}^{small}$ elastic sessions in Cell- i , the elastic sessions cannot get their peak rates, but a certain slowdown is necessary. From this it is now easy to calculate the number of allocated sub-carriers to elastic sessions in each system state:

$$\begin{aligned} U_{i,e} \cdot l_{i,e}^* + (U_{i,r} - U_{i,r}^{RiI}) \cdot l_r &= CH - RiI; \\ U_{i,e} &= (U_{i,e}^{small} + 1) \dots U_{i,e}^{MAX}. \end{aligned} \quad (5)$$

From which the number of sub-carriers allocated to elastic sessions:

$$\begin{aligned} l_{i,e}^* &= \frac{(CH - RiI) - (U_{i,r} - U_{i,r}^{RiI}) \cdot l_r}{U_{i,e}}; \\ U_{i,e} &= (U_{i,e}^{small} + 1) \dots U_{i,e}^{MAX}. \end{aligned} \quad (6)$$

Summarizing; the number of allocated sub-carriers to elastic sessions in each state is given by:

$$l_{i,e}^* = \begin{cases} l_e^{MAX} & \text{if } U_{i,e} \leq U_{i,e}^{small}, \\ \frac{(CH - RiI) - (U_{i,r} - U_{i,r}^{RiI}) \cdot l_r}{U_{i,e}} & \text{otherwise.} \end{cases} \quad i = 0, \dots, 1; \quad (7)$$

That is, in each system state $(U_{0,r}, U_{0,e}, U_{1,r}, U_{1,e})$ we now know the number of allocated sub-carriers to mobile stations in the exterior and interior areas of the cell, and in each state we also know the slowdown factor of the elastic sessions:

$$\begin{aligned} K0I(U_{0,r}, U_{0,e}, U_{1,r}, U_{1,e}) &= U_{0,r} \cdot l_r; \\ K0E(U_{0,r}, U_{0,e}, U_{1,r}, U_{1,e}) &= U_{0,e} \cdot l_{0,e}^*; \\ a_2(U_{0,r}, U_{0,e}, U_{1,r}, U_{1,e}) &= \frac{l_e^{MAX}}{l_{0,e}^*}, \end{aligned} \quad (8)$$

and

$$\begin{aligned} K1I(U_{0,r}, U_{0,e}, U_{1,r}, U_{1,e}) &= U_{1,r} \cdot l_r; \\ K1E(U_{0,r}, U_{0,e}, U_{1,r}, U_{1,e}) &= U_{1,e} \cdot l_{1,e}^*; \\ a_4(U_{0,r}, U_{0,e}, U_{1,r}, U_{1,e}) &= \frac{l_e^{MAX}}{l_{1,e}^*}. \end{aligned} \quad (9)$$

C. The Markovian Property

We now make use of the assumptions that the arrival processes are Poisson and the nominal holding times are exponentially distributed. The transitions between the system states are due to an arrival or a departure of a session of class- k in either Cell-0 or in Cell-1. The arrival rates are given by the intensity of the Poisson arrival processes. Due to the memoryless property of the exponential distribution, the departure rates from each state depend on the nominal holding time of the in-progress sessions and on the slowdown factor in that state. Specifically, when the slowdown factor of a session of class- k is $a_k(U_{0,r}, U_{0,e}, U_{1,r}, U_{1,e})$, its departure rate is $\mu_k/a_k(U_{0,r}, U_{0,e}, U_{1,r}, U_{1,e})$.

The Markovian property for such systems was observed and formally proven by Nunez Queija *et al.* [10]. It is also used by Massoulié and Roberts in [11], where the departure

rates of the birth-death process are modulated by the actual instantaneous bandwidth of elastic traffic. Thus, the system under these assumptions is a continuous time Markov chain (CTMC) whose state is uniquely characterized by the state vector $\underline{U} = (U_{0,r}, U_{0,e}, U_{1,r}, U_{1,e})$.

D. Determining the Performance Measures of Interest

Based on the considerations of the preceding subsections, the performance measures of interest can be derived using the following observation. (The details of this reasoning along with rigorously deriving the performance measures are provided in [4].) The generator matrix of the CTMC can be determined taking into account that the death rates of the CTMC must be multiplied by the slowdown rates in each state. With the generator matrix in hand, the performance measures follow [4].

E. Numerical Examples

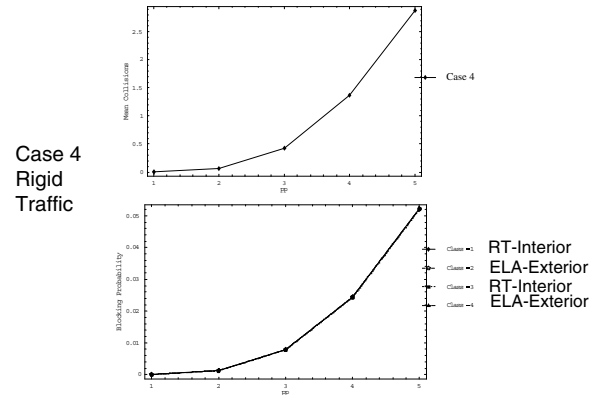


Fig. 4. Coordinated sub-carrier allocation without reuse partitioning when all traffic classes are peak allocated. The figure shows the mean number of collisions and the class-wise blocking probabilities as functions of the arrival intensity (being the same for all classes). At the highest load these values reach 3 and 5% respectively.)

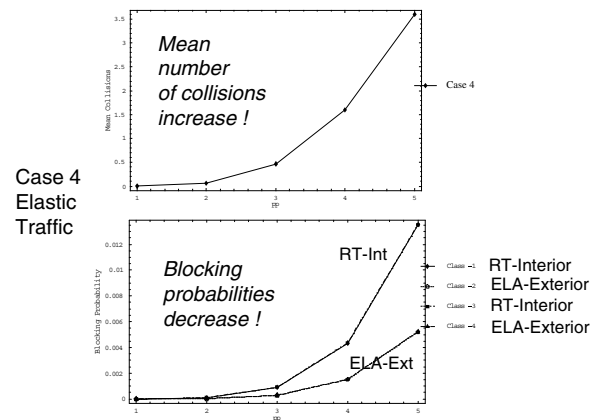


Fig. 5. Coordinated sub-carrier allocation without reuse partitioning when one of the service classes in each cell is elastic. The elastic sessions now experience a very low 0.5% blocking probability and also the real time sessions' blocking probability decreases to 1.5%. However, the mean number of collisions increases to 3.5.

We compare two extreme cases in terms of the number of barred sub-carriers. Figures 4-7 present results for the Reuse-1 case ($R0 = R1 = 0$), while Figures 8-9 concern the case when the collision zone is zero ($R0 = R1 = CH/2$). In all figures, the arrival intensity increases along the x axis. In the Reuse-1 case, when one of the service classes is elastic, the blocking probabilities decrease (both without and with reuse partitioning), but the mean number of collisions increases. This is because in the presence of elastic traffic the average resource utilization and the number of allocated sub-carriers increases. With higher reuse it is possible to eliminate the collisions (both with and without reuse partitioning) but at the expense of high blocking rate. However, when reuse partitioning is used, the blocking probabilities can be "brought back" to normal values, if one of the classes tolerate some slowdown. Therefore, the numerical results shown in Figures 8-9 are strong cases for reuse partitioning.

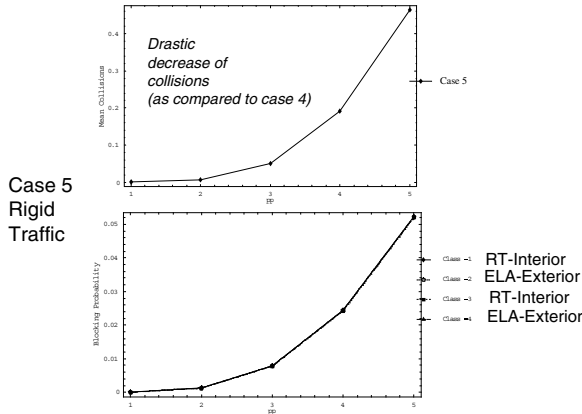


Fig. 6. Coordinated sub-carrier allocation with reuse partitioning when all service classes are rigid. Reuse partitioning does not decrease the blocking probabilities (same as in Figure 4), but it helps reduce the mean number of collisions (here to 0.45), ($R0 = R1 = 0$).

IV. CALCULATING THE SIGNAL-TO-INTERFERENCE-AND-NOISE RATIO

In this Section we are interested in analyzing the impact of sub-carrier collisions on the signal-to-interference-and-noise-ratio (SINR). Such analysis is of interest on its own right, because the SINR level is one of the important inputs to link level analysis that aims to evaluate the packet, block and symbol loss rates.

To understand the other important motivation for the SINR analysis, recall that the reuse partitioning technique allows interior mobile stations to collide, basically not considering such collisions to be "real" collisions. Obviously, the impact of collisions on the SINR, however, depends on at least two factors: the location of the border line between the interior and exterior areas and the assigned power levels to sub-carriers when they are used for a mobile station within the interior or in the exterior area. In this paper we will assume that no dynamic power control is applied, but in the downlink different power

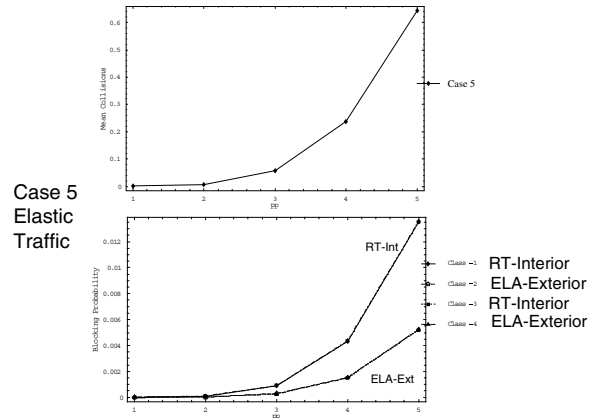


Fig. 7. Coordinated sub-carrier allocation with reuse partitioning when one of the service classes in each cell is elastic. The blocking probabilities again are the same as in the case without reuse partitioning (same as in Figure 5) and the mean number of collisions increases somewhat as compared to the rigid case ($R0 = R1 = 0$). (But it is still much lower than without reuse partitioning.)

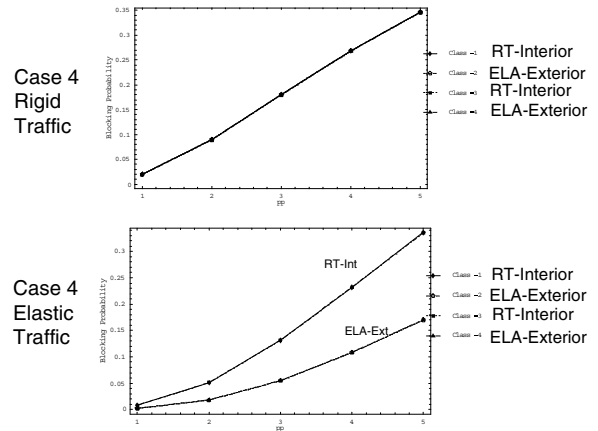


Fig. 8. Blocking probabilities without reuse partitioning when $R0 = R1 = CH/2$. The mean number of collisions is reduced to zero (not shown here), since the collision zone is now 0. However, the blocking probabilities become unacceptably high (over 30%) even when one of the service classes is elastic.

levels can be assigned to interior and exterior sub-carriers. Therefore, a SINR analysis as a function of the location of the colliding mobile stations and the assigned power levels provides important input to the actual dimensioning of the reuse partitioning technique.

Therefore, in this section we first present a simple path loss model that will be useful for the SINR model. Then, we summarize our finding in a proposition that states how the probability that the SINR remains under a predefined threshold depends on the location of the colliding mobile stations and on the applied sub-carrier power levels.

A. Path Loss Model for the Downlink

In this subsection we develop a path loss model that is based on the 3GPP technical report on propagation models [9]. The path loss between the i^{th} mobile station and the serving base

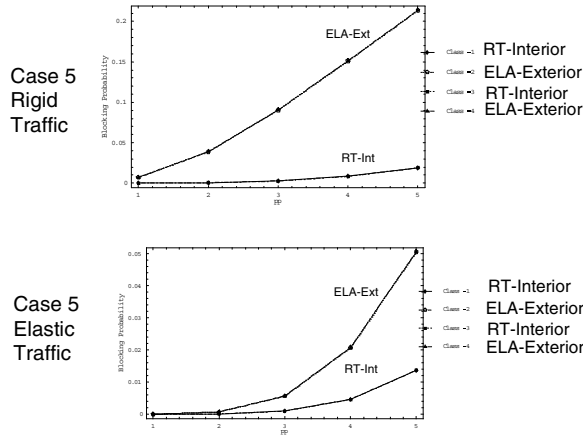


Fig. 9. Blocking probabilities with reuse partitioning when $R0 = R1 = CH/2$. The mean number of collisions is zero (not shown), and when one of the service classes is elastic, the blocking probabilities decrease drastically; to 5% (exterior sessions) and 1.5% (interior sessions).

station can be characterized as follows:

$$\varphi_i = r_i^\mu \cdot 10^{\frac{\varepsilon_i}{10}}.$$

According to this model, the path loss consists of two parts: the first part only depends on the distance (r) between the mobile and the base station; μ is a channel model dependent constant, typically between 2 and 4. The second part is due to the *shadowing*; here ν_i is assumed to be a lognormally distributed random variable of the form: $\nu_i = a \cdot \epsilon + b \cdot \varepsilon_i$; here a and b are taken $1/\sqrt{2}$. Furthermore, ϵ and ε are zero-mean random variables: $E[\epsilon] = E[\varepsilon_i] = 0$, $Var[\epsilon] = Var[\varepsilon_i] = \alpha^2$ and α has to be known (model input).

Let $\varepsilon \triangleq \varepsilon_0 - \varepsilon_1$, then the path loss ratio between two colliding base stations being at r_0 and r_1 distance from a given mobile station can be calculated as follows:

$$\frac{\varphi_0}{\varphi_1} = \left(\frac{r_0}{r_1}\right)^\mu \cdot 10^{\frac{\varepsilon_0 - \varepsilon_1}{10}} = \left(\frac{r_0}{r_1}\right)^\mu \cdot 10^{\frac{b \cdot (\varepsilon_0 - \varepsilon_1)}{10}} = \left(\frac{r_0}{r_1}\right)^\mu \cdot 10^{\frac{b \cdot \varepsilon}{10}} \quad (10)$$

It follows from the definition that ε is assumed to be a zero mean Gaussian random variable with standard deviation $\sqrt{2}\alpha$:

$$\varepsilon \sim N(0, \sigma^2) = N(0, \sqrt{2}\alpha).$$

B. Calculating the SINR Level in Case of Collisions for the Downlink

Proposition 1: Let θ be a predefined threshold and let $\xi \triangleq \frac{r_0}{r_1}$ be a random variable representing the ratio between the mobile station distances from its serving and disturbing base station respectively. Then, the probability that the SINR remains under this threshold is as follows.

$$Pr\left(\frac{P_0/\varphi_0}{P_1/\varphi_1 + N_0} < \theta\right) = \int_0^{Max[\xi]} (f_\xi(x)g(x))dx;$$

$$g(x) \triangleq \frac{1}{2} \operatorname{erfc}\left(-\frac{1}{2b\alpha} \cdot \left(\frac{x^\mu \theta}{P_0/P_1}\right)^{[dB]}\right).$$

where $f_\xi(x)$ is the probability density function of ξ .

Proof:

$$Pr\left(\frac{P_0/\varphi_0}{P_1/\varphi_1 + N_0} < \theta\right) = Pr\left(\frac{P_0}{\theta} < \frac{\varphi_0}{\varphi_1} \cdot P_1 + \varphi_0 \cdot N_0\right)$$

$$= Pr\left(\frac{P_0}{\theta} < \left(\frac{r_0}{r_1}\right)^\mu \cdot 10^{\frac{\varepsilon_0 - \varepsilon_1}{10}} \cdot P_1 + \varphi_0 \cdot N_0\right) \approx$$

$$\approx Pr\left(\frac{P_0}{\theta} < \xi^\mu \cdot \eta^\mu\right),$$

where

$$\eta \triangleq 10^{\frac{b \cdot \varepsilon}{10\mu}} \cdot \sqrt[4]{P_1} = \text{Random variable as a function of } \varepsilon.$$

Furthermore, let $M \triangleq \left(\frac{P_0}{\theta}\right)^{1/\mu}$. Then,

$$Pr\left(\frac{P_0/\varphi_0}{P_1/\varphi_1 + N_0} < \theta\right) = Pr\left(\frac{P_0}{\theta} < \xi^\mu \cdot \eta^\mu\right) =$$

$$= Pr(M < \xi \cdot \eta). \quad (11)$$

The probability that the multiple of two random variables exceeds a predefined value is straightforward to calculate:

$$Pr(M < \xi \cdot \eta) = \int_0^{Max[\xi]} \left(f_\xi(x) \underbrace{\int_{\frac{M}{x}}^{\infty} f_\eta(y) dy}_{\text{underbrace}} \right) dx.$$

Focusing on the part within the underbrace:

$$Pr\left(\eta > \frac{M}{x}\right) = Pr\left(10^{\frac{b\varepsilon}{10\mu}} \cdot \sqrt[4]{P_1} > \frac{\left(\frac{P_0}{\theta}\right)^{\frac{1}{\mu}}}{x}\right) =$$

$$= Pr\left(\frac{b\varepsilon}{10\mu} + \frac{1}{\mu} \cdot \log P_1 > \frac{1}{\mu} \cdot \log P_0 +$$

$$+ \frac{1}{\mu} \cdot \log\left(\frac{1}{\theta}\right) - \log x\right) =$$

$$= Pr\left(\varepsilon > \underbrace{\frac{10}{b} \log \frac{P_0/P_1}{\theta x^\mu}}_{\triangleq T}\right) = Pr(\varepsilon > T). \quad (12)$$

This means that we seek the probability that a Gaussian random variable exceeds a predefined value:

$$Pr(\varepsilon > T) = \frac{1}{2} \operatorname{erfc}\left(\frac{1}{\sqrt{2}\sigma^2} \cdot T\right) =$$

$$= \frac{1}{2} \operatorname{erfc}\left(-\frac{5}{b\alpha} \cdot \log \frac{x^\mu \theta}{P_0/P_1}\right) = g(x). \quad (13)$$

Substituting back to (11) completes the proof:

$$Pr(M < \xi \cdot \eta) =$$

$$= \int_0^{Max[\xi]} \left(f_\xi(x) Pr\left(\eta > \frac{M}{x}\right) \right) dx =$$

$$= \int_0^{Max[\xi]} (f_\xi(x)g(x))dx.$$

■

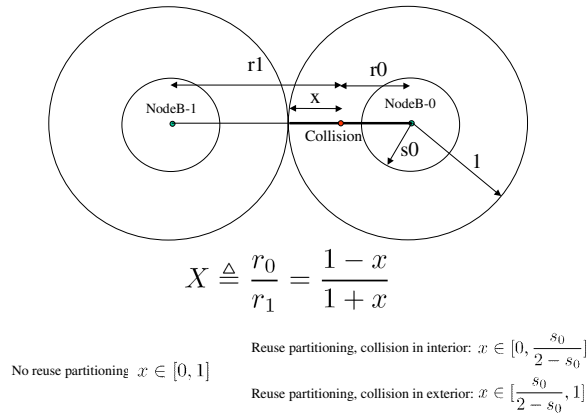


Fig. 10. A special case to calculate the density function of the ξ random variable. We choose a random point along the direct line between the two base stations within the cell under study, then the density of ξ takes the form of $\frac{2}{(1+x)^2 \cdot N}$, where the N normalization constant depends whether we consider the case without reuse partitioning or interior or exterior collisions in the case of reuse partitioning.

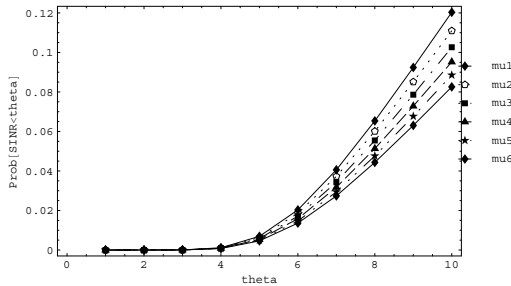


Fig. 11. Reference case: no reuse partitioning. Along the x axis we increase the θ threshold value; the y axis is the probability that the SINR value is below this value. The different curves correspond to different μ values in the path loss model (2...4.5). With greater μ the collision has less impact on the SINR.

C. Numerical Examples for Downlink Traffic

Equation (11) is useful, because it provides an easy means to calculate the probability that the SINR remains under a certain threshold if one knows the density function of $\xi = \frac{r_0}{r_1}$. This $f_\xi(x)$ depends on the user distribution over the coverage area of the two cells that we are studying. In practice, the $f_\xi(x)$ could come from simulation and/or measurements. To illustrate the impact of the parameters of the reuse partitioning method on the SINR given that a collision occurs, let us use an $f_\xi(x)$ as illustrated by Figure 10. The normalization constant that guarantees that the $f_\xi(x)$ is indeed a probability density for the three cases are: for the case without reuse partitioning: $N = 1$; for the case with reuse partitioning and choosing a point randomly in the inner circle: $N = s_0$; and for the case when we choose a random point in the exterior area of the cell: $N = 1 - s_0$. The results for the reuse partitioning are shown by Figures 12-13 (mobile station under study in the exterior area) and Figures 14-15 (mobile station under study in the interior area).

Figures 12-13 shows results for the case when the mobile

station in the cell under study is in the exterior area of the cell. The neighbor base station uses the same sub-carrier for a mobile station in the exterior area in its cell, and therefore the the power allocated for the colliding sub-carriers is the same. When s_0 is small, the SINR becomes a little worse than in the reference case (no reuse partitioning). This is because when s_0 is small, there is still a high chance that the mobile station in the cell under study is close to its serving base station. In contrast, as indicated in Figure 13, the SINR is severely degraded when s_0 is greater, because in this case, the mobile station is far from its base station and the interfering base station is closer. From the previous sections we know that greater s_0 means a greater interior and thereby a greater Reuse-1 area, which indicated the trade-off between the effective reuse and the SINR distribution for exterior mobiles.

Figures 14-15 consider the case when the mobile station under study is within the interior area of the cell. Here we focus on the case when this mobile station collides with a sub-carrier in the neighbor cell that is used for a mobile in the exterior area of that cell and therefore the interfering power is significantly greater than the power allocated to the interior mobile station under study. However, when s_0 is small (not shown in Figures), the SINR level is not seriously affected by collisions, since the mobile station is close to its base station, even in the worst case when this distance is s_0 and the interfering base station is $2 - s_0$ away.

In Figures 14-15 the radius of the inner circle is greater and therefore the SINR level is seriously affected by collisions, especially in the case when the interfering sub-carrier's power level is 6 times that of the mobile station's under study. It is clear that the radius of the interior area should not be chosen too great in order to protect the weaker inner mobile stations from the impact of collisions.

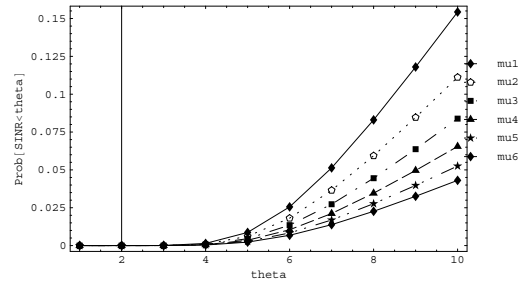


Fig. 12. SINR level at the mobile station under study when it is in the exterior area of the cell and s_0 is small (1/3). The interfering sub-carrier from the neighbor cell has the same power level. The SINR performance is either somewhat worse or somewhat better than without reuse partitioning depending on the μ parameter of the path loss model ($\mu = 2 \dots 4.5$).

V. CONCLUSIONS

This paper basically consists of three tightly inter-related parts that together give insight into the trade-offs inherent in a simple reuse partitioning scheme applicable for frequency

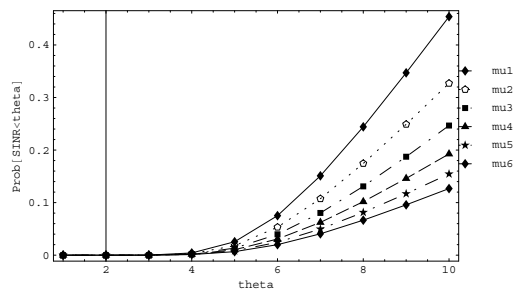


Fig. 13. SINR level at the mobile station under study when it is in the exterior area of the cell and s_0 is large (2/3). The interferer sub-carrier from the neighbor cell has the same power level. The SINR performance is much worse than without reuse partitioning and it depends much on the μ parameter of the path loss model ($\mu = 2 \dots 4.5$).

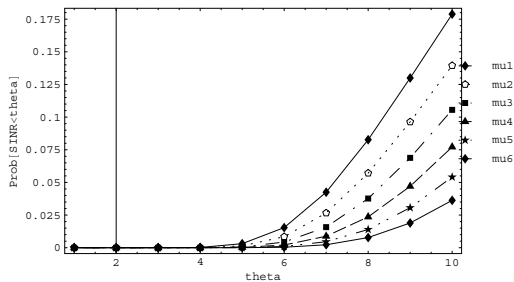


Fig. 14. SINR level at the mobile station under study when it is in the interior area of the cell and s_0 is large (2/3). The interferer sub-carrier from the neighbor cell has 3 times as high power level. The SINR performance compared to the reference case now depends on the μ parameter: when it is high (the interfering signal "fades away" faster), SINR is better than in the reference case, (i.e. no reuse partitioning, Figure 11) otherwise it is now worse than in the reference case.

divided systems. The first part evaluates the expected number of colliding sub-carriers *given* that the number of sub-carriers in the cell under study and in the dominant interfering cell is known. First, reuse partitioning significantly reduces the mean number of collisions if by collisions one only means the ones that have a noticeable impact on the SINR performance of the cell under study (that is collisions between mobile stations in the exterior area of the respective cells). Second, reuse partitioning increases the sub-carrier utilization since now all sub-carriers can be allocated (although some of them only to mobile stations in the interior area of the cell). The second part considered the case when sessions arrive according to a Poisson process at the cells and they may get blocked if the system cannot support their class-dependent resource requirements. In this dynamic setting, without reuse partitioning, the blocking probabilities become high (we considered an example where they were around 35%), but with reuse partitioning, especially in the presence of elastic traffic, the blocking probabilities are acceptable without increasing the expected number of collisions. In order to take advantage of the reuse partitioning policy, one needs to determine the border line between the interior and exterior cell areas and the proper power levels for sub-carriers must be determined. This issue was studied in the third part of the paper, where we proposed a methodology

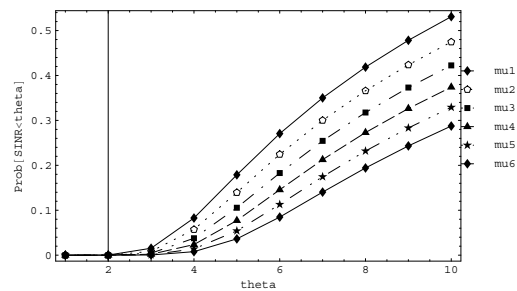


Fig. 15. SINR level at the mobile station under study when it is in the interior area of the cell and s_0 is large (2/3). The interferer sub-carrier from the neighbor cell has 6 times as high power level. The SINR performance compared to the reference case is always worse than in the reference case (i.e. no reuse partitioning, Figure 11), irrespective of the μ .

that can be used to study the tradeoff between the size of the interior cell and the SINR performance of mobile stations in the interior and exterior areas given that there is a collision with the dominant interferer cell.

From the static model it is clear that reuse partitioning increases the number of allocatable channels and reduces the mean number of collisions, both under the random and coordinated allocation policy. In the dynamic case these effects are even more pronounced: reuse partitioning can drastically reduce the class-wise blocking probabilities as compared to a non-partitioned system, especially in the presence of elastic traffic. However, reuse partitioning requires some design procedures to determine the partition borders and the assigned power levels on the down-link; we have provided a means to study the impact of these on the SINR performance of the system.

REFERENCES

- [1] 3GPP 25.814, "Evolved UTRA Physical Layer Aspects", 2005.
- [2] 3GPP TR 25.913, "Requirements for Evolved UTRA and Evolved UTRAN", 2005.
- [3] 3GPP Document, R2-052931, C-Plane Architecture for Long Term Evolved UTRA, available at: http://www.3gpp.org/ftp/tsg_ran/WG2_RL2/TSGR2_49/Documents/Joint%20RAN2-RAN3%20docs, 2005.
- [4] G. Fodor, "Performance Analysis of a Reuse Partitioning Technique for OFDM Based Evolved UTRA", *Technical Report*, April 2006.
- [5] E. Altman, "Capacity of Multi-service Cellular Networks with Transmission-Rate Control: A Queueing Analysis", *ACM Mobicom '02*, Atlanta, GA, September 23-28, 2002.
- [6] E. Altman, "Rate Control and QoS-related Capacity in Wireless Communications", - Keynote Speech at *Quality of Future Internet Services - QoFIS*, Stockholm, October 2003.
- [7] G. Fodor and M. Telek, "Performance Analysis of the Uplink of a CDMA Cell Supporting Elastic Services", in the Proc. of *IFIP Networking 2005*, Waterloo, Canada, Springer LNCS 3462, pp. 205-216, 2005.
- [8] Mathias Johansson, "Dynamic Reuse Partitioning Within Cells Based on Local Channel and Arrival Rate Fluctuations", *Technical Report*, Uppsala University, Sweden, 2005. <http://www.signal.uu.se/Staff/mj/pub/intercell.pdf>
- [9] 3GPP TR 25.942, Radio Frequency System Scenarios, 2005.
- [10] R. Nunez Queija, J. L. van den Berg, M. R. H. Mandjes, "Performance Evaluation of Strategies for Integration of Elastic and Stream Traffic", *International Teletraffic Congress*, UK, 1999.
- [11] L. Massoulie and J. Roberts, "Bandwidth Sharing: Objectives and Algorithms", *INFOCOM 1999*. Available at: <http://www-sop.inria.fr/mistral/pub/massoulie.html>.